J Mol Med (2016) 94:1229–1240
DOI 10.1007/s00109-016-1449-5

JMolMed

ORIGINAL ARTICLE

Mitochondrial aldehyde dehydrogenase 2 deficiency aggravates energy metabolism disturbance and diastolic dysfunction in diabetic mice

Cong Wang[1] · Fan Fan[1] · Quan Cao[1] · Cheng Shen[1] · Hong Zhu[1] · Peng Wang[1] · Xiaona Zhao[1] · Xiaolei Sun[2] · Zhen Dong[3] · Xin Ma[2] · Xiangwei liu[1] · Shasha Han[1] · Chaoneng Wu[1] · Yunzeng Zou[1,2] · Kai Hu[1] · Junbo Ge[1,2] · Aijun Sun[1,2]

Received: 8 March 2016 / Revised: 12 July 2016 / Accepted: 18 July 2016 / Published online: 3 August 2016

Abstract
Diabetes causes energy metabolism disturbance and may lead to cardiac dysfunction. Mitochondrial aldehyde dehydrogenase 2 (ALDH2) protects cardiac function from myocardial damage. Therefore, understanding of its roles in diabetic heart is critical for developing new therapeutics targeting ALDH2 and mitochondrial function for diabetic hearts. This study investigated the impact of ALDH2 deficiency on diastolic function and energy metabolism in diabetic mice. Diabetes was induced in ALDH2 knockout and wild-type mice by streptozotocin. Cardiac function was determined by echocardiography. Glucose uptake, energy status, and metabolic profiles were used to evaluate cardiac energy metabolism. The association between ALDH2 polymorphism and diabetes was also analyzed in patients. Echocardiography revealed preserved systolic function and impaired diastolic function in diabetic ALDH2-deficient mice. Energy reserves (phosphocreatine/adenosine triphosphate ratio) were reduced in the diabetic mutants and were associated with diastolic dysfunction. Western blot analysis showed that diabetes induces accumulated lipid peroxidation products and escalated AMP-activated protein kinase–LKB1 pathway. Further, ALDH2 deficiency exacerbated the diabetes-induced deficient myocardial glucose uptake and other perturbations of metabolic profiles. Finally, ALDH2 mutations were associated with worse diastolic dysfunction in diabetic patients. Together, our results demonstrate that ALDH2 deficiency and resulting energy metabolism disturbance is a part of pathology of diastolic dysfunction of diabetic hearts, and suggest that patients with ALDH2 mutations are vulnerable to diabetic damage.

Key Message

- ALDH2 deficiency exacerbates diastolic dysfunction in early diabetic hearts.
- ALDH2 deficiency triggers decompensation of metabolic reserves and energy metabolism disturbances in early diabetic hearts.
- ALDH2 deficiency potentiates oxidative stress and AMPK phosphorylation induced by diabetes via post-translational regulation of LKB1.
- Diabetic patients with ALDH2 mutations are predisposed to worse diastolic dysfunction.

Keywords Diastolic function · Diabetes · Energy metabolism · ALDH2

Cong Wang, Fan Fan and Quan Cao contributed equally to this work.

Electronic supplementary material The online version of this article (doi:10.1007/s00109-016-1449-5) contains supplementary material, which is available to authorized users.

✉ Junbo Ge
jbge@zs-hospital.sh.cn

✉ Aijun Sun
sun.aijun@zs-hospital.sh.cn

[1] Shanghai Institute of Cardiovascular Diseases, Zhongshan Hospital, Fudan University, Fenglin Road 180, Shanghai 200032, People's Republic of China

[2] Institute of Biomedical Science, Fudan University, Shanghai 200032, People's Republic of China

[3] Department of Cardiology, Huashan Hospital, Fudan University, Shanghai 200040, People's Republic of China

Introduction

Diabetes mellitus is associated with an increased risk of heart failure and diabetic cardiomyopathy [1, 2]. Diastolic

dysfunction is one of the earliest manifestations, which progresses to systolic dysfunction and finally to symptomatic heart failure in patients with diabetic cardiomyopathy [2], although structural or functional changes of the heart are hardly detectable in the early stages of diabetes. Several scenarios are postulated for the pathogenesis of diastolic dysfunction, including the formation of advanced glycation end products, titin-isoform switching, increased collagen accumulation, and abnormal myocytic calcium kinetics [3–5]; but the actual cause remains unknown. Metabolic disturbances in the diabetic heart are important hallmarks of the remodeling process that contributes to cardiac complications in diabetes. Accumulating evidence indicates interdependence between energy metabolism and diastolic dysfunction in diabetic hearts [6, 7].

Mitochondrial aldehyde dehydrogenase 2 (ALDH2) plays a critical role in acetaldehyde metabolism. Recent studies have suggested a beneficial role for ALDH2 in late diabetic cardiomyopathy in terms of systolic function and autophagy [8, 9]. However, whether diastolic function and energy metabolism were affected in the early stages of diabetic myocardial injury and if ALDH2 has a role in the process have not been addressed. Since the prevalence of diabetes is increasing dramatically, particularly in Asian countries and approximately 40 % of Asian people carry the ALDH2 mutant genotype and it is therefore of importance to explore the association between ALDH2 deficiency and metabolic disturbance/diastolic dysfunction in diabetic hearts. In the present study, we tested the hypothesis that ALDH2 deficiency might be linked with energy metabolism disturbance and diastolic dysfunction in diabetic hearts.

ALDH2 knockout mice were used to demonstrate the impact of ALDH2 deficiency on diastolic function in diabetic mice. Given the indispensible role of energy metabolism in the pathogenesis of diabetic heart, present study examined the energy metabolism disturbance from various aspects including cardiac glucose uptake, energy reserve, metabolomics as well as LKB1–AMPK energy regulatory axis. To further elucidate the effect of ALDH2 deficiency on cardiac function with diabetes background, we examined the association between ALDH2 polymorphism and cardiac dysfunction in 118 diabetic patients from a population-based cohort.

Materials and methods

Animals and diabetes model

All procedures were approved by the Institutional Animal Care and Use Committee of Fudan University. Adult male C57BL/6 mice (12 weeks old) and same genetic background ALDH2 knockout mice (KO) were used for this study. Experimental diabetes was induced by daily intraperitoneal administration of 45 mg/kg streptozotocin (STZ) freshly dissolved in sodium citrate buffer (pH 4.5) for 5 days. Control mice were injected with sodium citrate buffer. Three weeks after STZ injection, mice were killed. Blood glucose levels were monitored weekly until the time of being killed. Mice with fasting blood glucose levels >13 mM were considered as having diabetes.

Echocardiography and Doppler analysis

Transthoracic echocardiography (Vevo707B; Visual Sonics Inc., Toronto, ON, Canada) examination was carried out to evaluate cardiac geometry and function as described previously [10]. Briefly, parasternal long-axis and apical four-chamber views of the left ventricle (LV) were used to analyze systolic and diastolic function, respectively. The thickness of the interventricular septal and posterior walls, LV dimensions, LV ejection fraction, and fractional shortening were recorded in M-mode images to assess cardiac geometry and systolic function. Diastolic function was measured by transmitral Doppler flow E and A velocities, tissue Doppler imaging E′ velocities, and E-wave deceleration time. Measurements were made by two experienced technicians blinded to the groups and averaged from at least three cardiac cycles.

Histological examination

Hearts were arrested after anesthesia by ketamine and rapidly immersed in 4 % neutral formaldehyde or OCT compound (Tissue-Tek; Sakura Finetek Europe B.V., Alphen aan den Rijn, the Netherlands). Specimens embedded in paraffin were sectioned at a thickness of 4 μm and stained with hematoxylin and eosin and Masson's trichrome to assess myocardial morphology and cardiac collagen content, respectively. Frozen specimen was stained with Oil Red O and Periodic Acid Schiff (PAS) to assess cardiac neutral triglycerides and glycogen, respectively. Images were analyzed using Image-Pro Plus software (Media Cybernetics, Rockville, MD, USA).

Transmission electron microscopy (TEM) examination

Briefly, freshly dissected LV tissue was fixed with 2.5 % glutaraldehyde (pH 7.4) for at least 2 h. After three washes in 0.1 M phosphate buffer followed by fixation with 1 % osmium tetroxide, specimens were dehydrated in ethanol and ultrathin sections (50–60 nm) were cut on an ultramicrotome (Leica, Wetzlar, Germany) and stained with 3 % uranyl acetate and lead citrate. Images were acquired with a CM-120 microscope (Philips, Amsterdam, the Netherlands).

Measurement of cardiac energy status

Heart tissue stored at −80 °C was homogenized in lysis buffer consisting of methanol–water (60 % *v*/v) at −20 °C and

centrifuged, and the supernatant was analyzed by liquid chromatography (LC)/mass spectrometry (MS). Standards for adenosine triphosphate (ATP), adenosine diphosphate(ADP), (adenosine monophosphate) AMP, and phosphocreatine (PCr) were purchased from Sigma (St. Louis, MO, USA). An 1100 series binary high-performance LC system (Agilent Technologies, Waldbronn, Germany) combined with a 4000 QTRAP linear ion trap mass spectrometer (AB/MDS Sciex, Concord, ON, Canada) were used for differentiation and quantification of ATP, ADP, AMP, and PCr. MS data was analyzed using Analyst v.1.4 software (AB/MDS Sciex). Chromatographic separation was performed at 200 μl/min on a Hydro-RP(C18), 150 mm × 2.1 mm I.D., 4-μm particle column (Agilent Technologies, Santa Clara, CA, USA) with two eluents (10 mM tributylamine adjusted with 15 mM acetic acid or methanol) at room temperature. Absolute concentrations in tissue extracts were determined by the standard addition method to correct for matrix effects.

Positron emission tomography (PET)/computed tomography (CT) imaging

For micro-PET/CT analysis, mice that had fasted overnight were anesthetized with 5 % isoflurane and intravenously injected with fludeoxyglucose (18F-FDG; 11.76 ± 1.55 Mbq in 100 μl) prior to imaging; mice were scanned 45 min later (Inveon mPET/CT; Siemens, Knoxville, TN, USA). Image quality was improved by micro-CT anatomical alignment. Data were reconstructed with the three-dimensional ordered subset expectation maximization algorithm. Maximum standard uptake value (SUVmax) was determined as a measure of cardiac glucose uptake capacity, which was normalized to the body weight of mice and total injection dosage [11].

Metabolomics study

A 1-ml volume of methanol was added to 50 mg LV tissue, which was homogenized on ice followed by centrifugation at 14,000 rpm and 4 °C for 10 min. A C18 column (100 mm × 2.1 mm, 1.8 μm; Agilent Technologies, USA) and chromatography system (Agilent Technologies, USA) were used for MS. To determine global metabolic patterns and identify potential biomarkers, primary LC/MS data were subjected to multivariate statistical analyses, including principal component analysis, projections to latent structures discriminant analysis, and orthogonal partial least squares discriminant analysis (OPLS-DA) using SIMCA-P + 11 software (Umetric, Umea, Sweden). Variables were significant when their importance in the projection was >1 and the *P* value calculated from the Student's t test was <0.05.

Western blot analysis

Myocardial protein extraction and western blotting were performed as previously described [12] using antibodies against the following proteins: AMP-activated protein kinase (AMPK), phospho-AMPKα (Thr172), LKB1, phospho LKB1 (Ser428) (Cell Signaling Technology, Danvers, MA, USA), ALDH2 (Epitomics, Burlingame, CA, USA), and 4-hydroxynonenal (4HNE) (ab46545; Abcam, Cambridge, MA, USA). Horseradish peroxidase-conjugated secondary antibody was used (Kangchen Biotechnology, Nanjing, China). Band intensity of proteins of interest was normalized to that of glyceraldehyde 3-phosphate dehydrogenase (GAPDH).

Human ALDH2 polymorphism

Based on a population-based cohort from the Jinshan district of Shanghai, 118 individuals out of 1,503 residents were clinically diagnosed as having diabetes and underwent further extensive medical examinations, including Doppler echocardiography assessment, and blood specimen collection at the research center. The study protocol was approved by Fudan University Ethics Committee and all participants provided informed consent for participation in accordance with the Declaration of Helsinki (World Medical Association and R281). Eligibility criteria for subjects with diabetes were based on World Health Organization criteria. ALDH2 genetic polymorphisms were detected as previously described [13].

Statistical analysis

Data are expressed as mean ± SEM and were analyzed using SPSS v.16.0 for Windows (SPSS Inc., Chicago, IL, USA). Multi-group comparisons were carried out by one-way analysis of variance followed by post-hoc analysis. Correlation was evaluated with Pearson's correlation coefficient. The Student's t test was used to analyze associations between ALDH2 genotypes and cardiac function. *P* value <0.05 was considered statistically significant.

Results

General features of early diabetic heart

Blood glucose level was elevated in STZ-treated wild-type (WT-STZ) and knockout (KO-STZ) mice compared to non-diabetic mice 1 week after STZ injection. Notably, the increase was greater in KO than in WT mice (Fig. 1a). We next examined myocardial histology and ultrastructure in the diabetes model to access early structure alternations. Cardiomyocyte cross-sectional area was similar

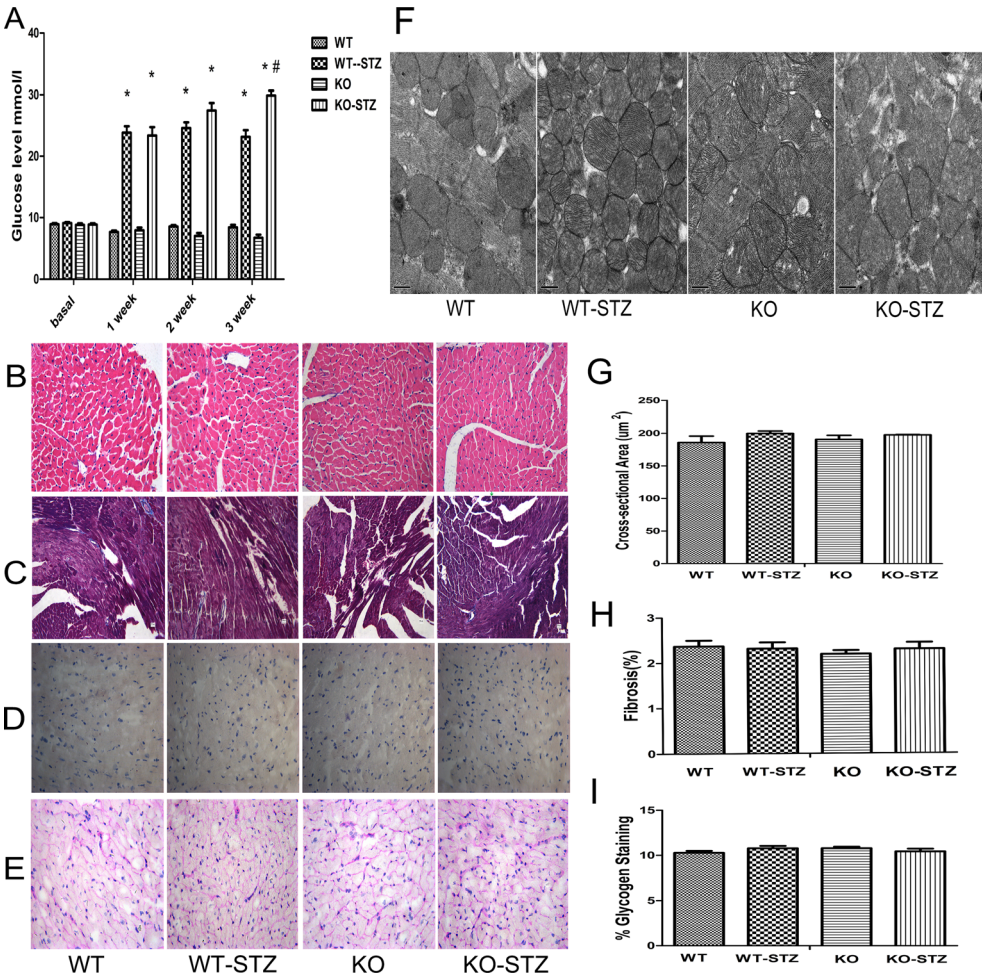

Fig. 1 General features of early diabetic heart. **a** Blood glucose levels in four groups of mice before and after STZ treatment. Values are expressed as mean ± SEM (n = 6–13 per group).*P < 0.05 vs. respective controls; $^{\#}P$ < 0.05 vs. WT-STZ. **b** Representative images of hematoxylin and eosin (HE) staining of transverse LV myocardial sections (×400). **c** Representative images of Masson's trichrome staining of myocardial sections (×200). **d** Oil Red O staining of myocardial sections (×400). **e** PAS staining showing glycogen in the myocardium (×400). **f** Representative TEM images of the LV in four groups of mice. *Scale bar*, 0.5 μm. Quantitative analysis of cardiomyocyte cross-sectional area (**g**), fibrosis (**h**), glycogen content (**i**) (mean ± SEM; n = 3–5 per group)

among the four groups (Fig. 1b, g); there was no difference in interstitial fibrosis detected by Masson's trichrome staining (Fig. 1 c, h). Accumulation of energy substrates was then evaluated by Oil Red O (Fig. 1d) and PAS staining (Fig. 1e) to visualize triglycerides and glycogen, respectively. The results showed that neither was affected by the ALDH2 deficiency nor by experimentally induced diabetes (Fig.1i). No obvious ultrastructure alteration among four groups was observed by TEM analysis (Fig.1f). Taken together, these results indicate no significant changes in myocardial histology and ultrastructure among four experimental groups.

ALDH2 deficiency impairs diastolic function

Echocardiography was performed to evaluate LV systolic and diastolic function. LV systolic function (fractional shortening and ejection fraction), and LV chamber size (LV end-diastolic and end-systolic dimensions) and ventricular thickness were similar among groups [Electronic supplementary material (ESM) Table S1]. Diastolic dysfunction (Fig. 2a) was evidenced in KO-STZ mice, as indicated by decreased E/A ratio and increased E/E′ratio, and prolonged deceleration time. (Fig. 2b–e). These results suggest that diastolic function was already impaired at the early stage of diabetes in KO-STZ mice, despite preserved systolic function in these mice.

Cardiac energy status at the early stage of diabetic mice

To assess the impact of ALDH2 on cardiac energy status in diabetes, the levels of ATP, ADP, AMP, and PCr were measured. Consistent with previous studies [14], ATP levels were similar among four experimental groups at the early stages of diabetes (Fig. 3a). In contrast, the ratios of ADP/ATP and AMP/ATP were significantly higher in KO-STZ mice than in KO mice (p = 0.032 and 0.017, respectively), whereas no difference was observed between WT and WT-STZ mice (Fig. 3b, e). On the other hand, PCr level and PCr/ATP ratio were decreased in KO-STZ mice, but not in WT-STZ mice (Fig. 3c, d). Of note, PCr/ATP ratio was positively correlated with E/A ratio (r = 0.525; p = 0.037) (Fig. 3f). Thus, energy

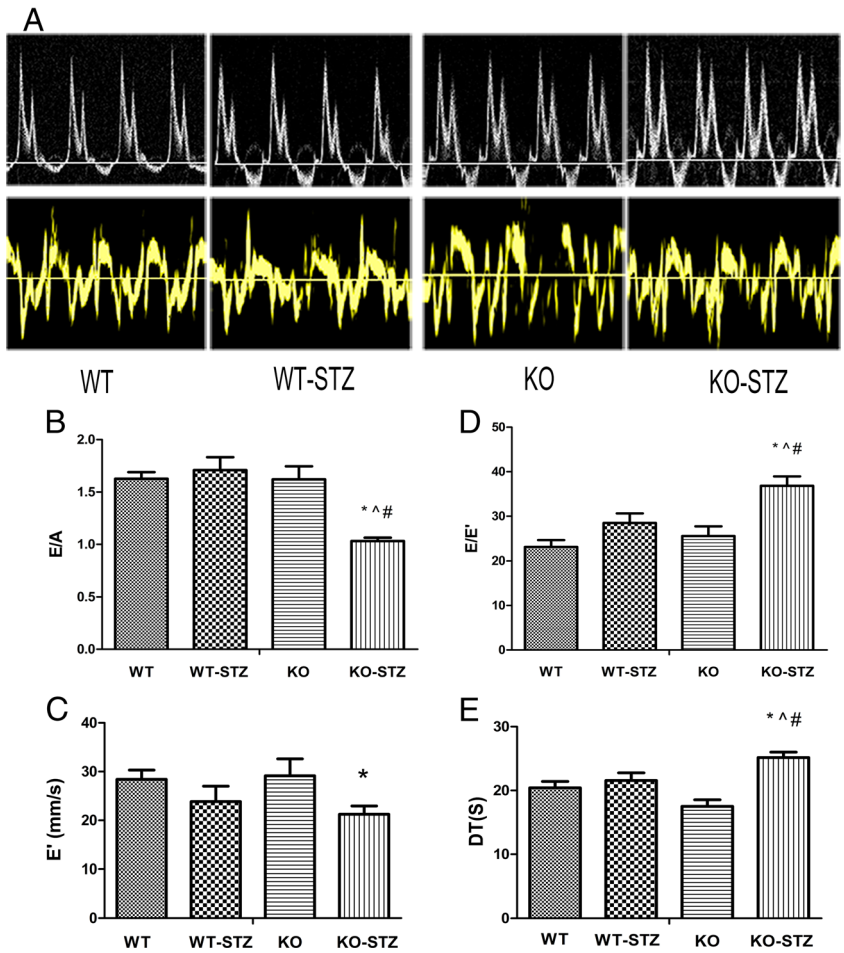

Fig. 2 Effect of STZ treatment on diastolic function in ALDH2 KO and WT mice.**a** Representative images of transmitral Doppler flow and tissue Doppler imaging. **b** Ratio of early and late transmitral inflow velocity, as measured by transmitral mitral Doppler (E/A). **c** Early diastolic mitral valve annulus velocity (E′ wave). **d** Ratio of early transmitral flow velocity to early diastolic mitral valve annulus velocity (E/E′). **e** Deceleration time (DT). Values are expressed as mean ± SEM ($n = 4$–7 per group). $^{*}P < 0.05$ vs. respective controls; $^{\#}P < 0.05$ vs. WT-STZ; $^{\wedge}P < 0.05$ vs. WT

metabolism of KO-STZ mice is impaired in the early diabetic stage.

ALDH2 deficiency reduces myocardial glucose uptake

To further scrutinize myocardial metabolism, glucose uptake was quantified by micro-PET. Under basal conditions, myocardial 18F-FDG uptake was similar between WT and KO mice. However, glucose uptake was decreased in both WT-STZ and KO-STZ hearts compared to the respective non-diabetic controls (Fig. 4a). Maximum standard uptake value (SUVmax) was 1.3-fold lower in WT-STZ mice than in WT mice, but the difference was not statistically significant (Fig.4b) and SUVmax was significantly lower in KO-STZ mice compared to WT-STZ mice ($P = 0.011$) (Fig. 4b). These results indicate that myocardial glucose uptake is reduced in the diabetic WT mice and which is further exacerbated in diabetic ALDH2 KO mice. However, considering the insulin changes, the decreased glucose uptake may not be caused directly by local myocardial ALDH2 deficiency.

ALDH2 deficiency activates AMPK signaling and increases lipid peroxidation

AMPK signaling and oxidative stress play important roles in cardiac energy metabolism [15–17]. Therefore, the expression of AMPK signaling components and their phosphorylation status were evaluated. Western blot analysis of LV tissues revealed accumulation of the lipid peroxidation product-4HNE in KO-STZ mice, suggesting diabetes induced oxidative stress; while ALDH2 expression was significantly downregulated in WT-STZ mice under diabetic stress. (Fig. 5a–d.) Although myocardial AMPK expression level remained unchanged in cases of diabetes and ALDH2 deficiency (Fig. 5e, g.), AMPK phosphorylation was increased in WT-STZ mice, which was further enhanced in KO-STZ mice (Fig. 5h, i). To determine the related mechanism, the expression and phosphorylation of LKB1 (Fig. 5f), an upstream regulator of AMPK signaling, was evaluated. LKB1 phosphorylation was significantly increased in WT-STZ mice, and which was further augmented in KO-STZ mice (Fig. 5k, l), while the total level of LKB1 was similar among

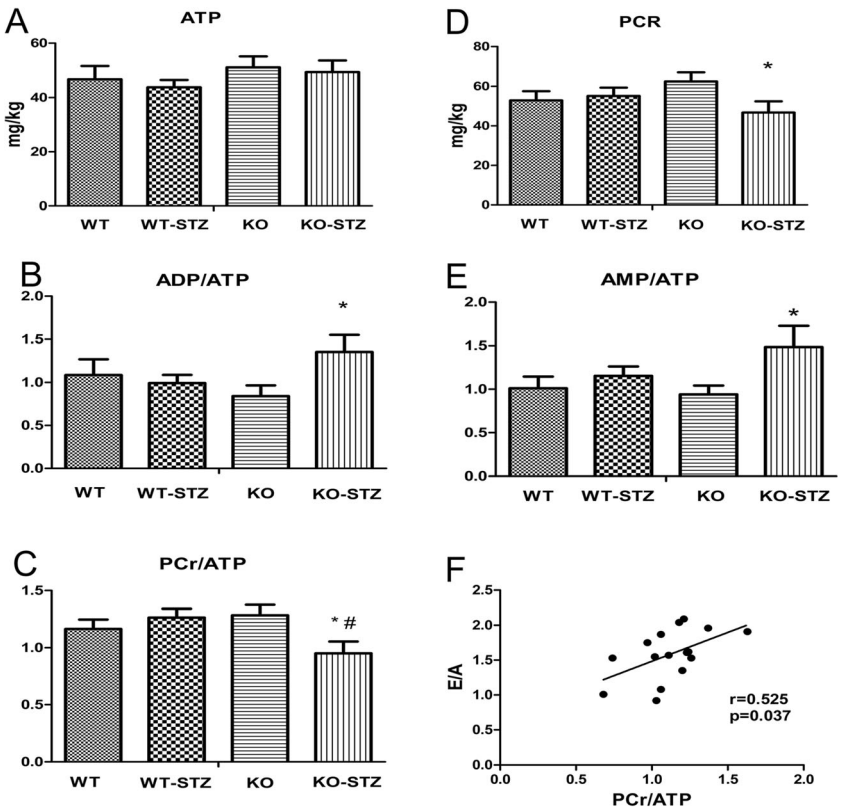

Fig. 3 Cardiac energy status in control and diabetic heart tissue as determined by MS. **a** Quantitative analysis of ATP levels. **b–c** Ratios of ADP/ATP (**b**) and PCr/ATP (**c**). **d** Quantitative analysis of PCr levels. **e** Ratio of AMP/ATP. **f** Correlations between PCr/ATP and indices of diastolic function (E/A). Values are expressed as mean ± SEM (n = 5–9 per group). *P < 0.05 vs. respective controls; #P < 0.05 vs. WT-STZ

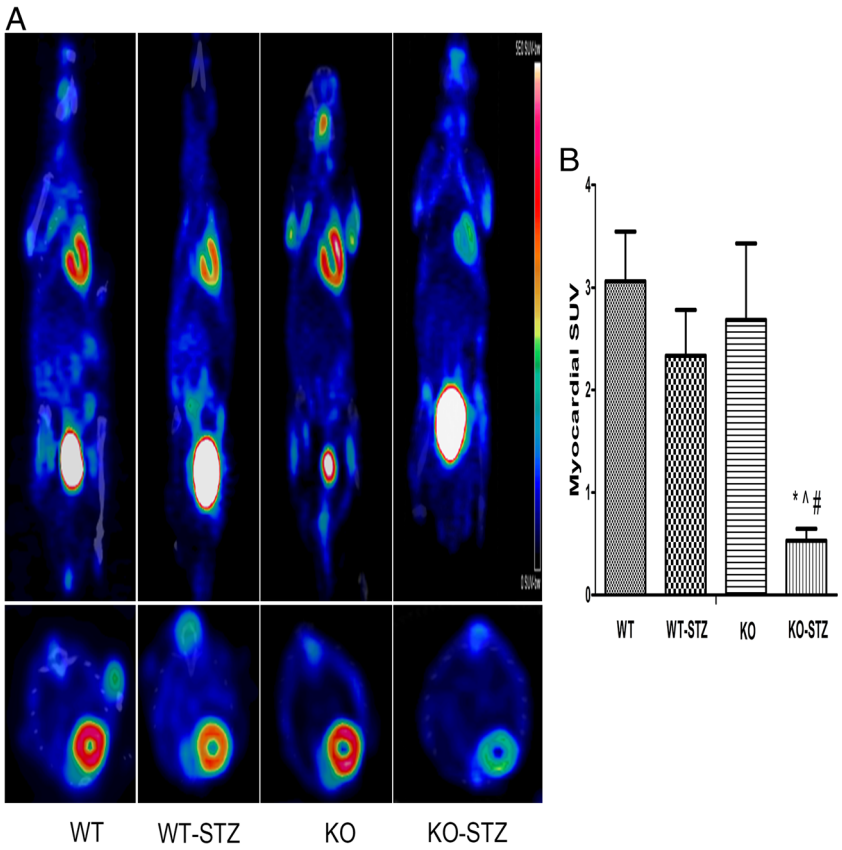

Fig. 4 Effect of ALDH2 deficiency and diabetes on myocardial glucose uptake. **a** Representative images of myocardial glucose uptake, as determined by micro-PET using 18F-FDG. **b** Myocardial glucose uptake SUV_{max} for four groups of mice. SUV_{max} was normalized to the total amount of radioisotope injected and the body weight of mice. Values are expressed as mean ± SEM (n = 4–6 per group). *P < 0.05 vs. respective controls; #P < 0.05 vs. WT-STZ; ^P < 0.05 vs. WT

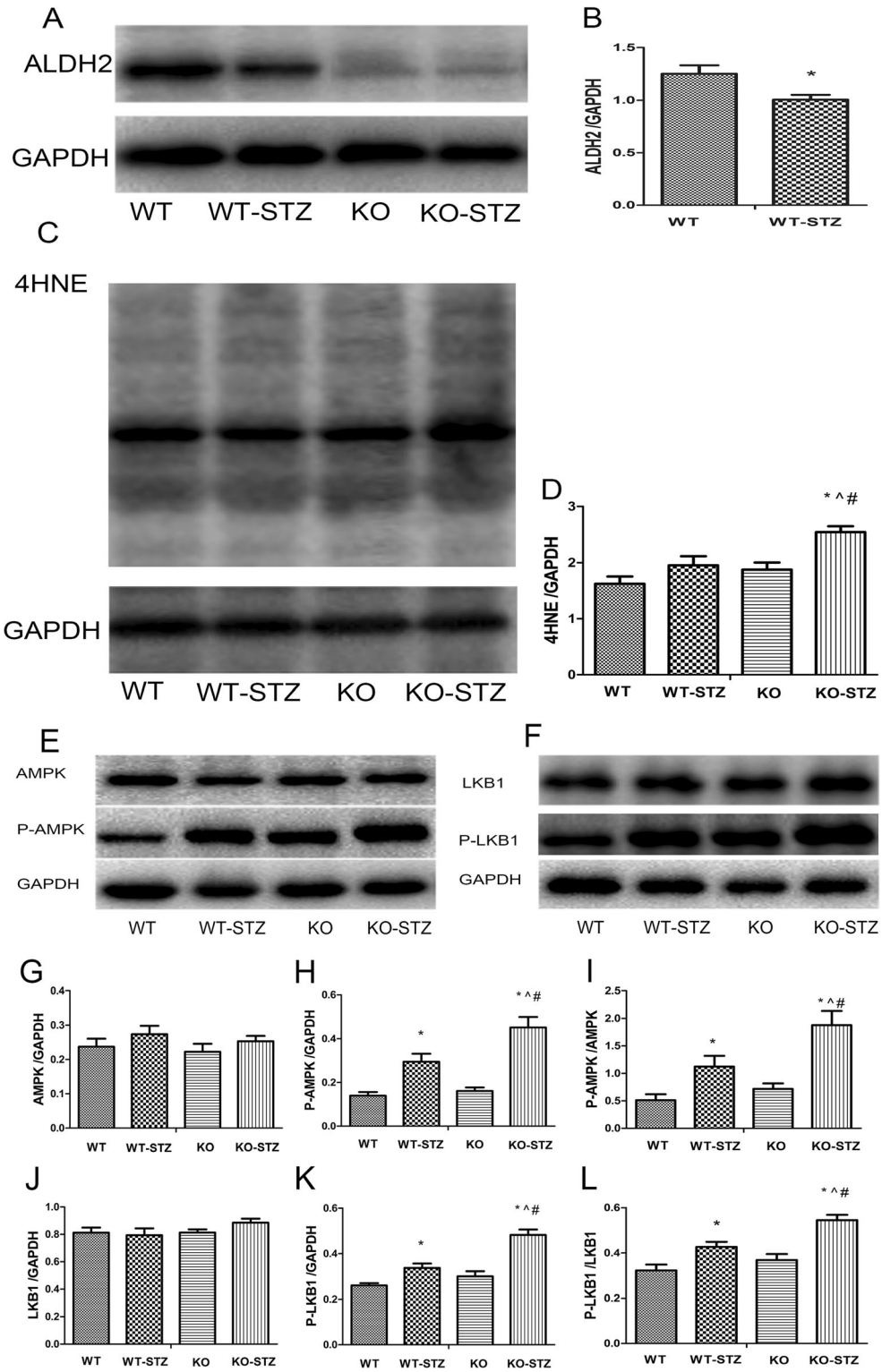

Fig. 5 Western blot analysis of ALDH2, 4HNE expression levels, and AMPK–LKB1 signaling components in diabetic and non-diabetic WT and ALDH2 KO mice. Representative blots of ALDH2 (**a**), 4HNE(**c**), and glyceraldehyde 3-phosphate dehydrogenase (GAPDH) (loading control). **b** ALDH2 expression. **d** 4HNE expression. (n = 4–6 per group). **e, f** Representative blots of AMPK and p-AMPK (**e**) and LKB1 and p-LKB1 (**f**) expression; glyceraldehyde 3-phosphate dehydrogenase (GAPDH) served as a loading control. **g** AMPK expression. **h** p-AMPK expression. **i** p-AMPK/AMPK ratio. **j** LKB1expression. **k** p-LKB1 expression. **l** p-LKB1/LKB1 ratio. Values are expressed as mean ± SEM (n = 3–8 per group). $^{*}P < 0.05$ vs. respective controls. $^{\#}P < 0.05$ vs. WT-STZ; $^{\wedge}P < 0.05$ vs. WT

groups (Fig. 5j). These results indicate that ALDH2 deficiency increases diabetes-induced oxidative stress and AMPK phosphorylation via post-translational regulation of LKB1 protein.

Metabolic profiling in response to diabetes and ALDH2

A global metabolomic analysis of LV tissue was performed in order to gain more comprehensive insight on the impact of

diabetes and ALDH2 on metabolic profiles (Fig. 6a, b). Diabetes resulted in profound metabolic profile changes related to the metabolism of fatty acids, amino acids, purine and pyrimidine nucleotides, and phospholipids (Fig. 6c and ESM Table S2). Specially, fatty acids metabolism was significantly perturbed. Levels of several carnitines, including 4,8 dimethylnonanoyl, trans-hexadec-2-enoyl, palmitoyl-L, and linoleyl carnitine, were increased in the diabetic mice compared to the control mice. Moreover, several diabetes-associated markers were also observed in the diabetic mice, including arachidonic acid, L-glutamine and stearic acid. Significantly, KO-STZ mice had more dysregulated glucose homeostasis and purine nucleotide metabolism, as evidenced by increased levels of glycocholic acid and decreased levels of inosine and hypoxanthine. Additionally, riboflavin and PGD2 were more increased in KO-STZ mice, indicating that endogenous protective mechanism was activated. Differences of various phospholipid metabolites, including phosphatidic acid (PA), phosphatidylserine (PS), phosphatidylcholine (PC), phosphatidylglycerol (PG), phosphatidylinositol (PI), phosphatidylethanolamine (PE), were detected between diabetic and non-diabetic mice, suggesting that phospholipids

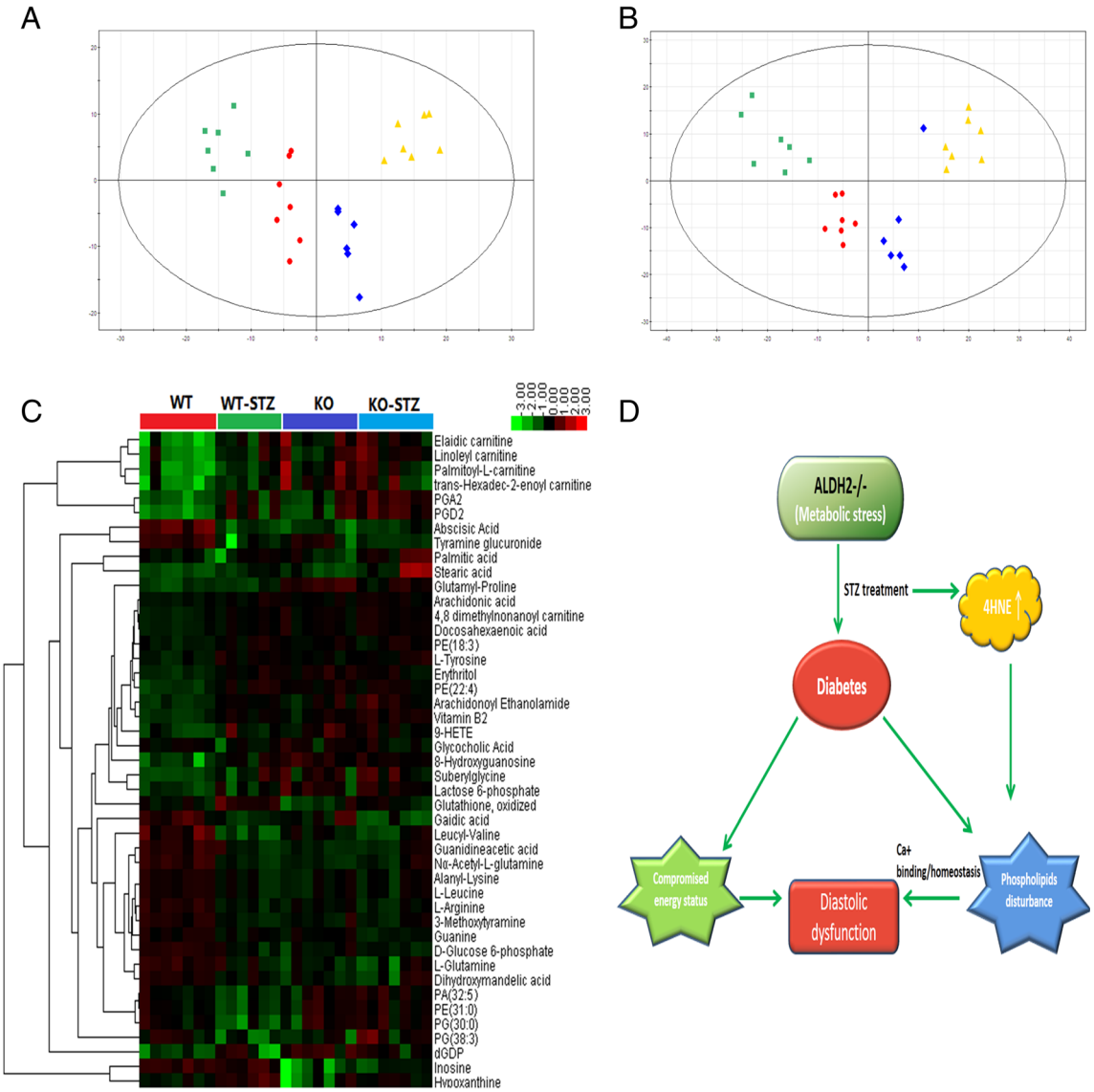

Fig. 6 **a, b** Effect of ALDH2 deficiency and diabetes on myocardial metabolomic profiles. OPLS-DA scores for WT and ALDH2 KO mice with or without diabetes in positive (**a**) and negative modes (**b**). *Yellow triangles*, WT; *blue squares*, WT-STZ; *green squares*, KO; *red circles*, KO-STZ. **c** Cardiac metabolome of WT and ALDH2 KO mice with or without diabetes. Heat map represents significant 45 metabolites among four groups and hierarchical clustering was applied. *Red color* denotes increase; *green color*, decrease. *Black color* indicates no change. **d** A schematic diagram of the effect of ALDH2 deficiency on diastolic function and energy metabolism in the early diabetic mice. ALDH2 deficiency triggers metabolic stress and exacerbates STZ-induced diabetic development, consequently resulted in significantly compromised energy status, 4HNE accumulation and phospholipids disturbance. The resulting energy metabolism disturbance per se or other mechanisms (like Ca^{+} binding, phospholipid homeostasis) finally may lead to diastolic dysfunction

metabolism was altered by diabetes (ESM Table S3). Of note, although the main affected metabolic pathways were similar between the two diabetic groups, the accumulation of phospholipids was more significant in KO-STZ mice compared to WT-STZ mice (ESM Table S3).

Above observations demonstrate that although there were no phenotypic differences between WT and KO mice, some metabolic pathways were significantly perturbed in KO-STZ mice. ALDH2 KO and diabetic mice share some similar metabolic changes, such as increased levels of diabetes risk markers: riboflavin, carnitine, L-tyrosine, arachidonic acid, and phospholipids.

Diabetic patients with ALDH2 mutations are predisposed to worse diastolic dysfunction

A total of 118 subjects, who were clinically diagnosed as diabetes from a population-based cohort, were included in this study. Since mutant genotypes (GA and AA) of ALDH2 indicate loss of ALDH2 function, and the number of AA genotype was too small to evaluate the effects of this genotype on the cardiac function changes in diabetic patients. Subjects with the GA and AA genotypes were grouped as GA + AA in the subsequent analysis.

The frequency of the normal GG genotype was 59.32 % ($n = 70$), and that of GA + AA genotype was 40.68 % ($n = 48$). The clinical characteristics of the two groups are shown in Table 1. Age, gender, BMI, hypertension, TG (triglycerides), CHOL (total cholesterol), LDL, and HDL were similar between the two groups (Table 1). Echocardiography examinations showed that LV dimension, LV wall thickness, and LV systolic function were similar between the two groups. However, the velocity of E wave was significantly lower in subjects with GA and AA genotypes than subjects with GG genotype (58.25 ± 2.15 vs 66.20 ± 1.51, $p < 0.05$). While, the velocity of A wave was significantly higher in subjects with GA and AA genotypes than in subjects with GG genotype (95.75 ± 2.39 vs 89.59 ± 1.39, $p < 0.05$). The E/A ratio was significantly lower in subjects with GA and AA genotypes than subjects with GG genotype (0.61 ± 0.02 vs 0.75 ± 0.02, $p < 0.05$). Similarly, E/E′ ratio was significantly higher in subjects with GA and AA genotypes than subjects with GG genotype (8.86 ± 0.36 vs. 7.72 ± 0.19, $p < 0.05$). Thus, diabetic patients with ALDH2 mutations predisposed to worse diastolic dysfunction, despite similar systolic function and cardiac dimension between the two groups (Table 2).

Table 1 Clinical characteristics of the subjects stratified by ALDH2 genotype

Variable	ALDH2 (GG) $N = 70$	ALDH2 (GA + AA) $N = 48$	*P* value
Age(years)	72.17 ± 0.66	73.54 ± 0.80	NS
Gender(male/female)	26/44	16/32	NS
BMI(kg m^{-2})	24.86 ± 0.39	25.82 ± 0.75	NS
Hypertension (%)	62.69	63.83	NS
TG (mmol l^{-1})	1.64 ± 0.13	2.07 ± 0.20	NS
CHOL (mmol l^{-1})	5.00 ± 0.10	5.15 ± 0.12	NS
LDL (mmol l^{-1})	2.90 ± 0.07	3.01 ± 0.10	NS
HDL (mmol l^{-1})	1.39 ± 0.04	1.33 ± 0.04	NS

TG triglycerides, *CHOL* total cholesterol, *NS* not significant

Discussion

The present findings indicate that ALDH2 deficiency exacerbates diastolic dysfunction and energy metabolism disturbances in the early disease stage of diabetic mice (Fig. 6d). ALDH2 deficiency also triggers metabolic stress and diabetic patients with ALDH2 mutations are predisposed to diastolic dysfunction. These findings suggest that ALDH2 deficiency aggravates cardiac abnormalities and energy metabolism disturbances in diabetic hearts.

Our data revealed that ALDH2 deficiency impairs diastolic function while systolic function and myocardial morphology remains normal in early disease stage of diabetes. This finding is in agreement with previous report in that LV diastolic dysfunction was found to be the first hallmark of diabetic cardiomyopathy, preceding the onset of systolic dysfunction [2, 7]. Our results also showed that metabolic reserves are decompensated in KO-STZ mice, in that PCr/ATP ratio was decreased in KO but not in WT diabetic mice. Indeed, myocardial PCr/ATP ratio is not only a sensitive index of the energetic state of the heart, but also correlates with cardiac function and outcome [18–20]. When workload or stress is increased,

Table 2 The effect of ALDH2 genotype on cardiac function in diabetic patients

Variable	ALDH2 (GG) $N = 70$	ALDH2 (GA + AA) $N = 48$	*P* value
LVEDD (mm)	46.42 ± 0.66	45.94 ± 0.79	NS
LVESD (mm)	29.06 ± 0.43	29.00 ± 0.51	NS
IVST (mm)	9.34 ± 0.15	9.79 ± 0.22	NS
PWT (mm)	9.22 ± 0.13	9.25 ± 0.16	NS
LVEF	67.56 ± 0.40	66.68 ± 0.67	NS
E (cm/s)	66.20 ± 1.51	58.25 ± 2.15	<0.05
A (cm/s)	89.59 ± 1.39	95.75 ± 2.39	<0.05
E/A	0.75 ± 0.02	0.61 ± 0.02	<0.05
DT (ms)	191.96 ± 5.02	191.09 ± 8.09	NS
E/E′	7.72 ± 0.19	8.86 ± 0.36	<0.05

LVEDD left ventricular end-diastolic dimension, *LVESD* left ventricular end-systolic dimension, *IVST* interventricular septal thickness, *PWT* posterior wall thickness, *LVEF* left ventricular ejection fraction, *DT* deceleration time

metabolic reserves in the heart are activated to meet increased energy demand [21]. This is reflected by a constant PCr/ATP ratio in physiological status. However, when the heart moves closer to decompensation, the ratio decreases and eventually with a decrement of ATP concentration [21–23]. In our study, although the ATP level is unaltered, energy status is compromised in KO-STZ mice, indicated by the increase in AMP/ATP and ADP/ATP ratios. Since ATP content is not considered as a sensitive or early index of energy depletion, it may underscore the importance of ATP turnover and other energy markers such as PCr/ATP. Our data suggest that mitochondrial ALDH2 has a permissive role in releasing metabolic reserves in response to hyperglycemic stress. Although our data do not confirm a causal relationship between diastolic dysfunction and energy depletion, it confirms a significant relationship between PCr/ATP ratio and E/A peak, as previously reported [24]. Because diastolic process is slower and consumes more energy than the systolic process, diastolic dysfunction may therefore precede systolic dysfunction upon energy depletion [18, 25]. It is thus reasonable to speculate that ALDH2 deficiency induces decompensation of metabolic reserves and concomitant deterioration of diastolic function.

The distinct metabolic phenotype of the diabetic heart includes a reduction in glucose uptake and increased fatty acid utilization [26]. Our 18F-FDG myocardial SUVmax data demonstrate that diabetes reduce glucose uptake in vivo, also consistent with previous findings [26, 27]. In early diabetic hearts which have high glucose levels induced AMPK and LKB1 phosphorylation, the condition worsened by ALDH2 deficiency. This finding strongly suggests that ALDH2 deficiency disturbs the energy metabolism (increased AMP/ATP, ADP/ATP, and decreased PCr/ATP ratios), which in turn, induces the activation of energy regulatory LKB1/AMPK pathway. In contrast, previous studies have indicated decreased AMPK phosphorylation in the diabetic heart [8]. The discrepancy might be explained by the differences in the dose and time of STZ administration, followed by different severities and molecular presentations of diabetes. It is known that AMPK is a sensor of cellular and whole-body energy status. AMPK activation is a complex process, including increased levels of ADP and AMP and decreases in ATP and upstream kinase phosphorylation [15, 16]. In the current study, diabetes induced the phosphorylation of the upstream kinase LKB1 in both WT-STZ and KO-STZ mice, with higher levels in the latter. In addition, ADP/ATP and AMP/ATP ratios are increased in KO-STZ mice. Based on these findings, we propose that AMPK activation is mediated by LKB1 in response to increases in the cellular ADP/ATP and AMP/ATP ratios in KO-STZ mice.

Our study also demonstrates that phospholipids accumulation is significantly increased in the diabetic ALDH2 knockout mice. These results are in agreement with previous studies demonstrating accumulation of phopholipids in the diabetic myocardium may contribute to diastolic dysfunction [28, 29]. Higher PC and PI levels are present in heart tissue with diastolic dysfunction [29], which is also a critical finding in this study. Concurrently, the product of lipid peroxidation-4HNE increase is more significant in KO-STZ mice, indicating more severe oxidative stress in these mice. Heart is a highly oxidative organ and myocardial plasmalemma and mitochondria contain large amounts of unsaturated phospholipids, which are susceptible to peroxidation in the heart [30]. Lipid peroxidation can greatly alter the physicochemical properties of membrane lipid bilayers, resulting in cellular dysfunction. Indeed, 4HNE is not only a kind of product of lipid peroxidation but also highly reactive with phospholipids. It can induce further damage to the plasma membrane, mitochondria, endoplasmic reticulum and finally result in cardiac dysfunction [31]. Although the underlying mechanisms responsible for diastolic dysfunction remain illustrated, several hypotheses, involving lipotoxicity, Ca2+ binding, altered sterol regulatory element-binding protein activity have been proposed [30, 32]. It is noteworthy that the heart has an antioxidant and detoxification system to block this vicious metabolic cycle, and ALDH2 exerts its vitally beneficial effects by reducing the load of toxic aldehydes such as 4-HNE. Our observation that ALDH2 deficiency increases oxidative stress and induces diastolic dysfunction, supports this notion, and we speculate that ALDH2 modulates diastolic function by maintaining phospholipid homeostasis.

Results from our metabolic profiling suggest that myocardial metabolites are significantly influenced by diabetes and ALDH2 deficiency. Our study also confirms several metabolic markers for diabetes, such as arachidonic acid [33], L-glutamine [34], and stearic acid [35], The altered levels of inosine, hypoxanthine and glycocholic acid in KO-STZ mice reflect inhibited purine nucleotide metabolism and worse glycaemia under the diabetic stress [36, 37]. Consistently, our data showed compensatory increase of riboflavin and PGD2 in KO-STZ mice, which have been considered as a protective mechanism to alleviate heart injury [38, 39]. Unexpectedly, our metabolomic analyses reveal a strikingly similarity between KO and diabetic mice, and suggest that ALDH2 deficiency leads to a metabolic stress phenotype. Our finding that ALDH2 exacerbates the effect of STZ-induced diabetics supports the hypothesis in that the perturbation in energy metabolism precedes structural and functional changes and predisposes the heart to cardiac abnormalities under stress. Importantly, our clinical data demonstrated worse diastolic dysfunction in diabetic patients with ALDH2 loss-of-function mutation genotype (GA and AA), despite similar systolic function and cardiac morphology compared to diabetic patients with GG genotype. This was in good consistency with our animal experimental results. Moreover, evidence from both experimental and clinical studies has revealed aberrations in metabolic profiles prior to the onset of

type 1 and 2 diabetes [40, 41]. Therefore, the manifestation of diastolic dysfunction and comprised energy state in KO-STZ mice may be explained by metabolic alterations induced by the ALDH2 deficiency.

Cardiac energy state and metabolic profiles are proposed to be more critical for sustaining cardiac function than substrate selection. However, fatty acids uptake was not measured in our study due to technical reasons. Therefore, we could not address this difference.

In conclusion, ALDH2 deficiency leads to the development of cardiac abnormalities in early diabetes. Our findings indicate that metabolic reserve decompensation and disturbance induced by the ALDH2 deficiency contribute to diastolic dysfunction and progression. Given that the diastolic dysfunction is a potentially reversible process [42, 43] and there are particularly high frequency of the ALDH2 loss-of-function allele mutation in Asian population [44, 45], our finding is of clinical implication in that screening ALDH2 mutation in diabetic patients and comprehensive therapy strategy may be a meaningful approach to alleviate and slow down the diabetic progression in this population.

Acknowledgment The authors acknowledge Liming Wei (the Institute of Biomedical Science, Fudan University) for technical support. This work was supported by National Natural Science Foundation of China (81570224; 81521001).

Compliance with ethical standards This study was carried out in accordance with the Guide for the Care and Use of Laboratory Animals, Eighth edition (2011). All procedures were approved by the Institutional Animal Care and Use Committee of Fudan University. The human polymorphism protocol was approved by Fudan University Ethics Committee and all participants provided informed consent for participation in accordance with the Declaration of Helsinki (World Medical Association and R281).

Conflict of interest The authors declare no competing financial interests.

References

1. Dhingra R, Vasan RS (2012) Diabetes and the risk of heart failure. Heart Fail Clin 8:125–133. doi: 10.1016/j.hfc.2011.08.008
2. Goyal BR, Mehta AA (2013) Diabetic cardiomyopathy: pathophysiological mechanisms and cardiac dysfuntion. Hum Exp Toxicol 32:571–590. doi: 10.1177/0960327112450885
3. Falcao-Pires I, Hamdani N, Borbely A, Gavina C, Schalkwijk CG, van der Velden J, van Heerebeek L, Stienen GJ, Niessen HW, Leite-Moreira AF, et al. (2011) Diabetes mellitus worsens diastolic left ventricular dysfunction in aortic stenosis through altered myocardial structure and cardiomyocyte stiffness. Circulation 124:1151–1159. doi: 10.1161/CIRCULATIONAHA.111.025270
4. Kruger M, Babicz K, von Frieling-Salewsky M, WA L (2010) Insulin signaling regulates cardiac titin properties in heart development and diabetic cardiomyopathy. J Mol Cell Cardiol 48:910–916. doi: 10.1016/j.yjmcc.2010.02.012.
5. Lovelock JD, Monasky MM, Jeong EM, Lardin HA, Liu H, Patel BG, Taglieri DM, Gu L, Kumar P, Pokhrel N, et al. (2012) Ranolazine improves cardiac diastolic dysfunction through modulation of myofilament calcium sensitivity. Circ Res 110:841–850. doi: 10.1161/CIRCRESAHA.111.258251
6. Mori J, Basu R, McLean BA, Das SK, Zhang L, Patel VB, Wagg CS, Kassiri Z, Lopaschuk GD, Oudit GY (2012) Agonist-induced hypertrophy and diastolic dysfunction are associated with selective reduction in glucose oxidation: a metabolic contribution to heart failure with normal ejection fraction. Circ Heart Fail 5:493–503. doi: 10.1161/CIRCHEARTFAILURE.112.966705
7. Fontes-Carvalho R, Ladeiras-Lopes R, Bettencourt P, Leite-Moreira A, Azevedo A (2015) Diastolic dysfunction in the diabetic continuum: association with insulin resistance, metabolic syndrome and type 2 diabetes. Cardiovasc Diabetol 14:4. doi: 10.1186/s12933-014-0168-x.
8. Guo Y, Yu W, Sun D, Wang J, Li C, Zhang R, Babcock SA, Li Y, Liu M, Ma M, et al. (2015) A novel protective mechanism for mitochondrial aldehyde dehydrogenase (ALDH2) in type I diabetes-induced cardiac dysfunction: role of AMPK-regulated autophagy. Biochim Biophys Acta 1852:319–331. doi: 10.1016/j.bbadis.2014.05.017
9. Zhang Y, Babcock SA, Hu N, Maris JR, Wang H, Ren J (2012) Mitochondrial aldehyde dehydrogenase (ALDH2) protects against streptozotocin-induced diabetic cardiomyopathy: role of GSK3beta and mitochondrial function. BMC Med 10:40. doi:10.1186/1741-7015-10-40
10. Shen C, Wang C, Fan F, Yang Z, Cao Q, Liu X, Sun X, Zhao X, Wang P, Ma X, et al. (2015) Acetaldehyde dehydrogenase 2 (ALDH2) deficiency exacerbates pressure overload-induced cardiac dysfunction by inhibiting Beclin-1 dependent autophagy pathway. Biochim Biophys Acta 1852:310–318. doi: 10.1016/j.bbadis.2014.07.014
11. Tseng LT, Lin CL, Tzen KY, Chang SC, Chang MF (2013) LMBD1 protein serves as a specific adaptor for insulin receptor internalization. J Biol Chem 288:32424–32432. doi: 10.1074/jbc.M113.479527
12. Sun A, Cheng Y, Zhang Y, Zhang Q, Wang S, Tian S, Zou Y, Hu K, Ren J, Ge J (2014) Aldehyde dehydrogenase 2 ameliorates doxorubicin-induced myocardial dysfunction through detoxification of 4-HNE and suppression of autophagy. J Mol Cell Cardiol 71:92–104. doi: 10.1016/j.yjmcc.2014.01.002
13. Zhang Y, Mi SL, Hu N, Doser TA, Sun A, Ge J, Ren J (2014) Mitochondrial aldehyde dehydrogenase 2 accentuates aging-induced cardiac remodeling and contractile dysfunction: role of AMPK, Sirt1, and mitochondrial function. Free Radic Biol Med 71:208–220. doi: 10.1016/j.freeradbiomed.2014.03.018
14. Spindler M, Saupe KW, Tian R, Ahmed S, Matlib MA, Ingwall JS (1999) Altered creatine kinase enzyme kinetics in diabetic cardiomyopathy. A(31)P NMR magnetization transfer study of the intact beating rat heart. J Mol Cell Cardiol 31:2175–2189. doi: 10.1006/jmcc.1999.1044
15. Grahame HD (2014) AMP-activated protein kinase: a key regulator of energy balance with many roles in human disease. J Intern Med 276:543–559. doi: 10.1111/joim.12268
16. McCarty MF (2014) AMPK activation—protean potential for boosting healthspan. Age (Dordr) 36:641–663. doi: 10.1007/s11357-013-9595-y
17. Gomes KM, Campos JC, Bechara LR, Queliconi B, Lima VM, Disatnik MH, Magno P, Chen CH, Brum PC, Kowaltowski AJ, et al. (2014) Aldehyde dehydrogenase 2 activation in heart failure restores mitochondrial function and improves ventricular function and remodelling. Cardiovasc Res 103:498–508. doi: 10.1093/cvr/cvu125
18. Rider OJ, Francis JM, Ali MK, Holloway C, Pegg T, Robson MD, Tyler D, Byrne J, Clarke K, Neubauer S (2012) Effects of

catecholamine stress on diastolic function and myocardial energetics in obesity. Circulation 125:1511–1519. doi: 10.1161/CIRCULATIONAHA.111.069518
19. Neubauer S (2007) The failing heart—an engine out of fuel. N Engl J Med 356:1140–1151. doi: 10.1056/NEJMra063052
20. Neubauer S, Horn M, Cramer M, Harre K, Newell JB, Peters W, Pabst T, Ertl G, Hahn D, Ingwall JS, et al. (1997) Myocardial phosphocreatine-to-ATP ratio is a predictor of mortality in patients with dilated cardiomyopathy. Circulation 96:2190–2196. doi: 10.1161/01.CIR.96.7.2190
21. Carley AN, Taegtmeyer H, Lewandowski ED (2014) Matrix revisited: mechanisms linking energy substrate metabolism to the function of the heart. Circ Res 114:717–729. 10.1161/CIRCRESAHA.114.301863
22. Shen W, Asai K, Uechi M, Mathier MA, Shannon RP, Vatner SF, Ingwall JS (1999) Progressive loss of myocardial ATP due to a loss of total purines during the development of heart failure in dogs: a compensatory role for the parallel loss of creatine. Circulation 100:2113–2118. doi: 10.1161/01.CIR.100.20.2113
23. Beer M, Seyfarth T, Sandstede J, Landschutz W, Lipke C, Kostler H, von Kienlin M, Harre K, Hahn D, Neubauer S (2002) Absolute concentrations of high-energy phosphate metabolites in normal, hypertrophied, and failing human myocardium measured noninvasively with (31)P-SLOOP magnetic resonance spectroscopy. J Am Coll Cardiol 40:1267–1274. doi: 10.1016/S0735-1097(02)02160-5
24. Perseghin G, Lattuada G, De Cobelli F, Esposito A, Canu T, Ragogna F, Maffi P, Scifo P, Secchi A, Del MA, et al. (2012) Left ventricular function and energy homeostasis in patients with type 1 diabetes with and without microvascular complications. Int J Cardiol 154:111–115. doi: 10.1016/j.ijcard.2010.09.010
25. Maslov MY, Chacko VP, Hirsch GA, Akki A, Leppo MK, Steenbergen C, Weiss RG (2010) Reduced in vivo high-energy phosphates precede adriamycin-induced cardiac dysfunction. Am J Physiol Heart Circ Physiol 299:H332–H337. doi: 10.1152/ajpheart.00727.2009
26. Isfort M, Stevens SC, Schaffer S, Jong CJ, Wold LE (2014) Metabolic dysfunction in diabetic cardiomyopathy. Heart Fail Rev 19:35–48. doi: 10.1007/s10741-013-9377-8
27. Bodiga VL, Eda SR, Bodiga S (2014) Advanced glycation end products: role in pathology of diabetic cardiomyopathy. Heart Fail Rev 19:49–63. doi: 10.1007/s10741-013-9374-y
28. Sysi-Aho M, Ermolov A, Gopalacharyulu PV, Tripathi A, Seppanen-Laakso T, Maukonen J, Mattila I, Ruohonen ST, Vahatalo L, Yetukuri L, et al. (2011) Metabolic regulation in progression to autoimmune diabetes. PLoS Comput Biol 7:e1002257. doi: 10.1371/journal.pcbi.1002257
29. Christoffersen C, Bollano E, Lindegaard ML, Bartels ED, Goetze JP, Andersen CB, Nielsen LB (2003) Cardiac lipid accumulation associated with diastolic dysfunction in obese mice. Endocrinology 144:3483–3490. doi: 10.1210/en.2003-0242
30. Anderson EJ, Katunga LA, Willis MS (2012) Mitochondria as a source and target of lipid peroxidation products in healthy and diseased heart. Clin Exp Pharmacol Physiol 39:179–193. doi: 10.1111/j.1440-1681.2011.05641.x
31. Chapple SJ, Cheng X, Mann GE (2013) Effects of 4-hydroxynonenal on vascular endothelial and smooth muscle cell redox signaling and function in health and disease. Redox Biol 1:319–331. doi: 10.1016/j.redox.2013.04.001
32. Lim HY, Wang W, Wessells RJ, Ocorr K, Bodmer R (2011) Phospholipid homeostasis regulates lipid metabolism and cardiac function through SREBP signaling in drosophila. Genes Dev 25:189–200. doi: 10.1101/gad.1992411
33. Mourmoura E, Vial G, Laillet B, Rigaudiere JP, Hininger-Favier I, Dubouchaud H, Morio B, Demaison L (2013) Preserved endothelium-dependent dilatation of the coronary microvasculature at the early phase of diabetes mellitus despite the increased oxidative stress and depressed cardiac mechanical function ex vivo. Cardiovasc Diabetol 12:49. doi: 10.1186/1475-2840-12-49
34. Cheng S, Rhee EP, Larson MG, Lewis GD, McCabe EL, Shen D, Palma MJ, Roberts LD, Dejam A, Souza AL, et al. (2012) Metabolite profiling identifies pathways associated with metabolic risk in humans. Circulation 125:2222–2231. doi: 10.1161/CIRCULATIONAHA.111.067827
35. Ma W, JH W, Wang Q, Lemaitre RN, Mukamal KJ, Djousse L, King IB, Song X, Biggs ML, Delaney JA, et al. (2015) Prospective association of fatty acids in the de novo lipogenesis pathway with risk of type 2 diabetes: the cardiovascular health study. Am J Clin Nutr 101:153–163. doi: 10.3945/ajcn.114.092601
36. Liu Y, Yan X, Mao G, Fang L, Zhao B, Liu Y, Tang H, Wang N (2013) Metabonomic profiling revealed an alteration in purine nucleotide metabolism associated with cardiac hypertrophy in rats treated with thiazolidinediones. J Proteome Res 12:5634–5641. doi: 10.1021/pr400587y
37. Taylor DR, Alaghband-Zadeh J, Cross GF, Omar S, le Roux CW, Vincent RP (2014) Urine bile acids relate to glucose control in patients with type 2 diabetes mellitus and a body mass index below 30 kg/m^2. PLoS One 9:e93540. doi: 10.1371/journal.pone.0093540
38. Wang G, Li W, Lu X, Zhao X (2011) Riboflavin alleviates cardiac failure in type I diabetic cardiomyopathy. Heart Int 6:e21. doi: 10.4081/hi.2011.e21
39. Katsumata Y, Shinmura K, Sugiura Y, Tohyama S, Matsuhashi T, Ito H, Yan X, Ito K, Yuasa S, Ieda M, et al. (2014) Endogenous prostaglandin D2 and its metabolites protect the heart against ischemia-reperfusion injury by activating Nrf2. Hypertension 63:80–87. doi: 10.1161/HYPERTENSIONAHA.113.01639
40. Oresic M (2012) Metabolomics in the studies of islet autoimmunity and type 1 diabetes. Rev Diabet Stud 9:236–247. doi: 10.1900/RDS.2012.9.236
41. Meikle PJ, Wong G, Barlow CK, Weir JM, Greeve MA, MacIntosh GL, Almasy L, Comuzzie AG, Mahaney MC, Kowalczyk A, et al. (2013) Plasma lipid profiling shows similar associations with prediabetes and type 2 diabetes. PLoS One 8:e74341. doi: 10.1371/journal.pone.0074341
42. Lee CH, Hung KC, Chang SH, Lin FC, Hsieh MJ, Chen CC, Chu CM, Hsieh IC, Wen MS, Wu D (2012) Reversible left ventricular diastolic dysfunction on Doppler tissue imaging predicts a more favorable prognosis in chronic heart failure. Circ J 76:1145–1150. doi: 10.1253/circj.CJ-11-0929
43. Loffredo FS, Nikolova AP, Pancoast JR, Lee RT (2014) Heart failure with preserved ejection fraction: molecular pathways of the aging myocardium. Circ Res 115:97–107. doi: 10.1161/CIRCRESAHA.115.302929
44. Li H, Borinskaya S, Yoshimura K, Kal'Ina N, Marusin A, Stepanov VA, Qin Z, Khaliq S, Lee MY, Yang Y, et al. (2009) Refined geographic distribution of the oriental ALDH2*504Lys (nee 487Lys) variant. Ann Hum Genet 73(Pt 3):335–345. doi: 10.1111/j.1469-1809.2009.00517.x
45. Chen CH, Ferreira JC, Gross ER, Mochly-Rosen D (2014) Targeting aldehyde dehydrogenase 2: new therapeutic opportunities. Physiol Rev 94:1–34. doi: 10.1152/physrev.00017.2013